The Influence of the Pitch to Diameter Ratio (P/D) on a Novel Tidal Turbine Performance

IOP Conf. Series: Materials Science and Engineering **893** (2020) 012008 doi:10.1088/1757-899X/893/1/012008

The Influence of the Pitch to Diameter Ratio (P/D) on a Novel Tidal Turbine Performance

Roslynna Rosli[1], Rosemary Norman[2], and Mehmet Atlar[3]

[1] Universiti Teknologi Brunei, Bandar Seri Begawan BE 1410, Brunei Darussalam
[2] Newcastle University, Newcastle upon Tyne NE1 7RU, United Kingdom
[3] University of Strathclyde, Glasgow G4 0LZ, United Kingdom

E-mail: roslynna.rosli@utb.edu.bn

Abstract. Computational Fluid Dynamics (CFD) offers numerical modeling investigating the performance that can be used other than or in tandem with experimental investigation. In order to offer meaningful results, the grid sensitivity test or Grid Convergence Index are usually carried out to ensure the solutions converging. This paper presents both grid sensitivity test results and the GCI calculation of a same numerical model exercised to investigate the performance of a tidal turbine, the Hydro-Spinna, with different P/D ratio. The CGI calculation presented the fine grid relative error to be 2.34% for the power coefficient and 2.28% for the thrust coefficient at their optimal TSR respectively. It was found that turbine with lowest P/D ratio has the highest power and thrust coefficient as well as TSR operational range. The turbine with P/D = 0.43 gives a power coefficient of 0.32 at the optimal TSR of 2.25.

1. Introduction

1.1. Introduction

The development in renewable energy specifically tidal energy is steadily progressing with aim to increase the contribution of renewable energy resources. Added with the critical issue of climate change, the research and development of tidal energy technologies are definitely welcome. The European Marine Energy Centre (EMEC) [1] in Scotland offers a hub for the development of tidal and wave energy technologies with different prototypes deployed in real sea conditions. In addition, the potential of new tidal energy technologies can also be investigated with a smaller scaled model in laboratory facilities such as cavitation tunnels and towing tanks. Investigation using Computational Fluid Dynamics can also be performed offering a vast platform for investigation especially during the early stage of design.

The Hydro-Spinna is a tidal turbine designed by Michael Gilbert and developed at Newcastle University. The Hydro-Spinna turbine extends in the axial direction as illustrated in Figure 1 making the turbine more three dimensional than a typical horizontal axis turbine. In order to assess the power potential of the turbine, the influence of the pitch length on the turbine performance needs to be assessed first. Wen [2] calculated that a lower P/D produced higher power using Blade Element Momentum Theory (BEMT) with the assumption that the turbine is a thin actuator disc. In order to investigate this, a numerical model was developed to predict the power and thrust coefficients of the turbine.

1.2. Hydro-Spinna Turbine

The Hydro-Spinna turbine is a novel horizontal axis tidal turbine presenting a helicoidal blade spiraling around the main axis as shown in Figure 1. The blades possess a cardioidal shape as illustrated in [3]. The HS500 is a 500 mm diameter model of the Hydro-Spinna turbines with cardioid shaped leading and trailing edge. The extended description and detailed geometry of the Hydro-Spinna HS500 model can be found in [3, 4]. The key parameters of the three turbines investigated are given below in Table 1.

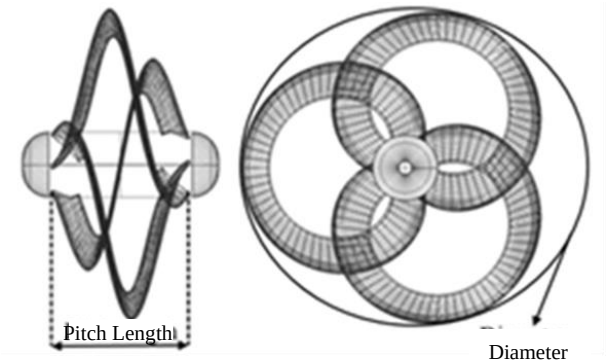

Figure 1. The Hydro-Spinna turbine parameters

Table 1. The turbine parameters with different P/D ratio

Pitch to Diameter Ratio, *P/D*	Diameter, D (mm)	Pitch, *P* (mm)	Pitch Angle at Root Section, β (Deg)	Hub Diameter, D_H (mm)
0.43	500	214	50.82	100
0.75		375	60.30	
1.00		500	68.11	

2. Numerical model

2.1. Reynolds-Averaged Navier Stokes Equations (RANS)

RANS and the continuity equations as defined in equations (1) and (2) were employed for the numerical model. RANS model is a modified Navier Stokes equation (3) taking the time averaged values of the fluctuating velocities and pressure variables to solve the equations. RANS was used due to its less computational time compared to Large Eddy Simulation models [5].

$$\frac{\partial(\rho\bar{V})}{\partial t} + \rho\left(\bar{V}.\vec{\nabla}\right)\bar{V} = -\vec{\nabla}.p + \mu\vec{\nabla}^2\bar{V} + \vec{\nabla}T_t + f_b \tag{1}$$

$$\frac{\partial\rho}{\partial t} + \nabla.(\rho V) = 0 \tag{2}$$

$$\frac{\partial(\rho V)}{\partial t} + \rho\left(V.\vec{\nabla}\right)V = -\vec{\nabla}.p + \mu\vec{\nabla}^2V + f_b \tag{3}$$

In addition, the hybrid Menter SST k-ω turbulence model is employed to consider the advantage of the k-ω at the near wall and k-ε in the fully turbulent region [6]. The Menter SST k-ω model are defined in equation (4) and (5) respectively.

$$\frac{\partial}{\partial t}(\rho k) + \nabla.(\rho k\bar{V}) = \nabla.\left[\left(\mu + \frac{\mu_t}{\sigma_k}\right)\nabla k\right] + P_k + \beta^*\rho k\omega \tag{4}$$

$$\frac{\partial}{\partial t}(\rho\omega) + \nabla.(\rho\omega\bar{V}) = \nabla.\left[\left(\mu + \frac{\mu_t}{\sigma_{\omega,1}}\right)\nabla\omega\right] + P_\omega - \beta_2\rho\omega^2 + 2\frac{\rho}{\sigma_{\omega,2}\omega}\frac{\partial k}{\partial x_k}\frac{\partial\omega}{\partial x_k} \tag{5}$$

2.2. Numerical domain

The numerical domain independency test was done where the dimension of 3D-8D-3D were found to be the optimal dimension. This means that inlet and outlet are 3D and 8D away from the centre of the

turbine respectively, whereas the radius of the cylindrical domain is at 3D from the centre of the turbine. The domain is divided into two parts i.e. the stationary and rotating domain where Moving Reference Frame was used for the rotating domain to represent the rotation of the turbine as shown in Figure 2. The rotating domain was set to be at 1.5D from the turbine centre, with the upstream and downstream boundaries set at 2D distance.

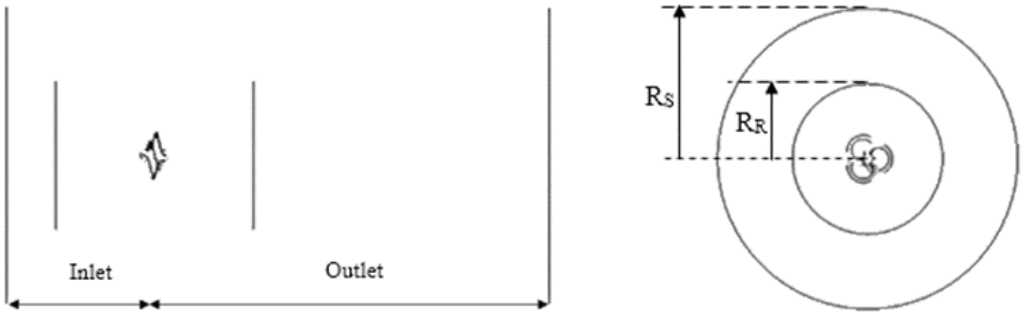

Figure 2. The numerical domain where inner vertical lines represent the upstream and downstream boundary of the rotating domain. R_R and R_S is the radius of the rotating and stationary domain respectively

2.3. Mesh independency test

The mesh independence analysis was conducted with the settings listed in Table 2 below. As mentioned previously, the domain dimensions for all model was set at 3D-8D-3D.

Table 2. Mesh settings of the numerical domain

Mesh Setting	Rotating (Rotating)	Stationary (Stationary)	Total
		Mesh Number	
1	1,439,663	216,322	1,655,985
2	1,847,224	216,322	2,063,546
3	1,847,224	355,116	2,202,340

2.4. Grid Convergence Index (GCI)

The numerical model was also validated using GCI where the procedure used in this paper is based on the widely accepted Richardson Extrapolation (RE) [7 -9] obtained from obtained from Celik et al [10] as described below.

Firstly, a representative mesh cell size, *h*, for three dimensional calculations is calculated as defined in equation (6).

$$h = \left[\frac{1}{N}\sum_{i=1}^{N}(\Delta V_i)\right]^{1/3} \tag{6}$$

where ΔV_i is the volume of the *i*th cell, and N is the total number of cells used in the computations.

Then, select three different sets of grids and run simulations to determine the value of the solutions for the study i.e. in this case power and thrust coefficients which is denoted as variable ϕ. The refinement factor $r = h_{coarse}/h_{fine}$ is recommended to be greater than 1.3. Let $h_1 < h_2 < h_3$ and $r_{21} = h_2/h_1,\ r_{32} = h_3/h_2$ and calculate the apparent order *p* of the method using equation (7) to (9).

$$p = \frac{1}{ln(r_{21})}|ln|\varepsilon_{32}/\varepsilon_{21}| + q(p)| \tag{7}$$

$$q(p) = ln\left(\frac{r_{21}^{p}-s}{r_{32}^{p}-s}\right) \tag{8}$$

$$s = 1.sgn(\varepsilon_{32}/\varepsilon_{21}) \tag{9}$$

where $\varepsilon_{32} = \emptyset_3 - \emptyset_2$, $\varepsilon_{21} = \emptyset_2 - \emptyset_1$ and $\emptyset_k$ represents the solution on the *k*th grid.

Calculate the grid convergence index as defined in equation (12) by first calculating the approximate relative error defined in equation (10) and the extrapolated relative error as defined in equation (11).

$$e_a^{21} = \left|\frac{\emptyset_1 - \emptyset_2}{\emptyset_1}\right| \tag{10}$$

$$e_{ext}^{21} = \left|\frac{\emptyset_{ext}^{12} - \emptyset_1}{\emptyset_{ext}^{12}}\right| \tag{11}$$

$$\mathrm{GCI}_{fine}^{21} = \frac{1.25 e_a^{21}}{r_{21}^p - 1} \tag{12}$$

3. Results and discussion

3.1. Validation of numerical model

The mesh sensitivity test considered three different sizes as indicated in Table 2. The results among the three settings were consistent with no significant difference as shown in Figure 3. The consistency in the mesh results was probably due to the small difference in the number of mesh with only a difference of approximately 200,000 cells between each setting. The results from the independency test presents a reliable numerical model for the turbine performance investigation. Similarly, other researchers also obtained optimum mesh numbers of approximately 2 million cells [11, 12]. In addition, the CGI calculation as shown in Table 3 resulted the numerical uncertainty for the fine-grid solution was 2.34% for the power coefficient and 2.28% for the thrust coefficient. Now that the numerical model has been validated both by using mesh sensitivity test and the GCI calculation, it is further used to investigated the performance of the turbine at different P/D ratio.

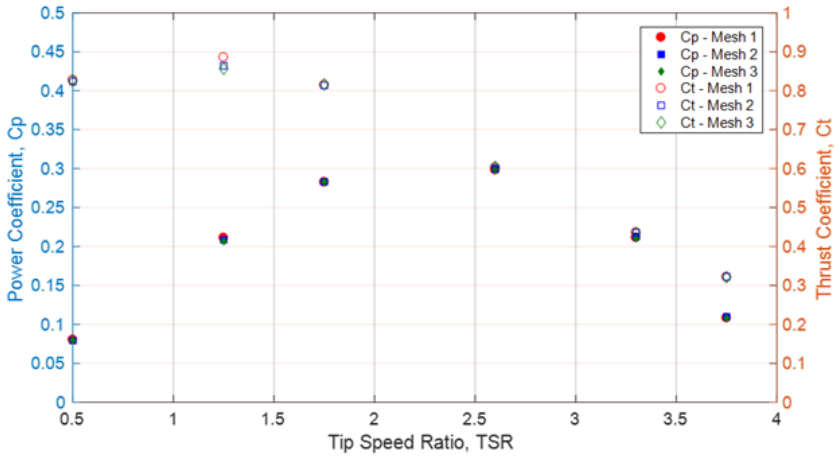

Figure 3. Mesh sensitivity result of the numerical model

Table 3. GCI results for the numerical model used

	ϕ = power coefficient at TSR = 2.6	ϕ = thrust coefficient at TSR = 1.75
N_1, N_2, N_3	2202340, 2063546, 1655985	
r_{21}	1.021	1.021
r_{32}	1.076	1.076
ϕ_1	0.2982	0.8144
ϕ_2	0.2991	0.8165
ϕ_3	0.2978	0.8136
p	7.173	6.355

e_a^{21}	0.0030	0.0026
e_a^{32}	0.0043	0.0036
$\mathbf{GCI}_{coarse}^{32}$	0.79%	0.75%
$\mathbf{GCI}_{fine}^{21}$	2.34%	2.28%

3.2. Turbine performance

The influence of the P/D ratio on the Power Coefficient (C_P) and Thrust Coefficient (C_T) was investigated for a full range of operational Tip Speed Ratio (TSR). The equations are defined below for reference.

$$C_P = \frac{Q\Omega}{0.5\,\rho A U^3} \tag{13}$$

$$C_T = \frac{T}{0.5\,\rho A U^2} \tag{14}$$

$$TSR = \frac{\Omega R}{U} \tag{15}$$

where Q is the torque, T is the thrust, Ω is the angular velocity of the turbine, ρ is the density of the fluid, A is the swept area of the turbine, and U is the flow velocity.

It was found that the P/D ratio greatly varies the performance characteristic of the turbine where the higher the ratio, the lower the power coefficient as shown in Figure 4. The results were found to be in agreement to the work conducted by Wen [2] where lower P/D gives the highest performance. The Hydro-Spinna turbine with P/D = 0.43 gives a power coefficient of 0.32 at the optimal TSR of 2.25. The operational range of this turbine is $0 < TSR < 4.15$. The higher the pitch length is the further the turbine is extended in the axial direction, while the diameter stays constant. Therefore, the higher the P/D ratio, the pitch angle of the turbine blade also increases hence contributing to the low power coefficient.

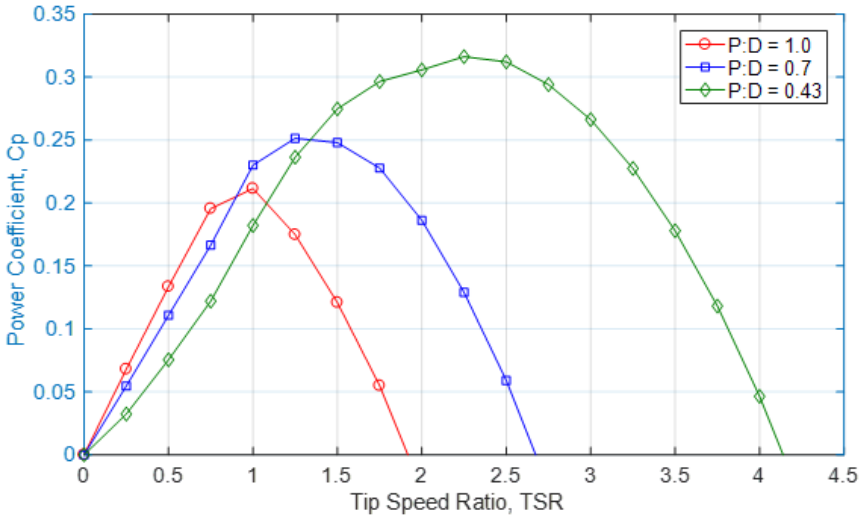

Figure 4. The power coefficient of the Hydro-Spinna turbine with different P/D ratio

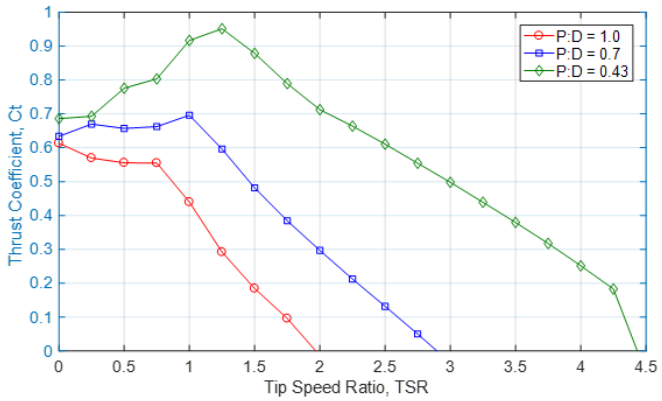

Figure 5. The thrust coefficient of the Hydro-Spinna turbine with different P/D ratio

In addition, it was also concluded that while the power increases with lower P/D the operational TSR range also increases. Where turbine with P/D ratio of 1 has a range of $0 < TSR < 1.9$. Hence, the Hydro-Spinna turbine with the lowest P/D ratio gives the highest power coefficient. Consequently, it also has the highest thrust coefficient among the three as presented in Figure 5. The turbine with P/D of 0.43 has a maximum thrust coefficient of 0.95 at TSR of 1.25, whilst at its optimal TSR i.e. TSR = 2.25, the thrust coefficient was only 0.66, 30% less than the maximum thrust. The high thrust at TSR = 0 is believed to be caused by the high solidity of the turbine surface blocking the current flow.

4. Conclusion

The performance characteristic of the Hydro-Spinna with different P/D ratio was successfully investigated by using a numerical model. The numerical model was validated by conducting domain and mesh sensitivity test as well as by GCI calculation. The numerical model validations were conducted to ensure the credibility of the model used. The numerical investigations concluded that that turbine with lowest P/D ratio has the highest power and thrust coefficient. Similarly, the operational *TSR* range of the turbines decreases with higher ratio.

5. References

[1] EMEC 2013 European Marine Energy Centre, Orkney, Scotland
[2] Wen Y. 2011 Optimisation and experimental validation of a novel marine turbine device. Newcastle University thesis.
[3] Rosli R, Norman R, and Atlar M 2014 GRAND Renewable, Tokyo, Japan, 30th July – 1st August 2014.
[4] Rosli R, Norman R, and Atlar M 2016 *Renewable Energy* **99** 1227-34.
[5] Breuer M, Jovičić N, and Mazaev K 2003 *International Journal for Numerical Methods in Fluids* **41(4)** 357-88.
[6] Menter FR 1996 *Journal of Fluids Engineering* **118(3)** 514-9.
[7] Roache PJ 2003 *Journal of Fluids Engineering* **125(4)** 731-2.
[8] NPARC Alliance 2008 NPARC Alliance CFD Verifications and Validation Website
[9] Ali MSM, Doolan CJ, and Wheatley V 2009 7th International Conference on CFD in the Minerals and Process Industries, Melbourne, Australia, 9th - 11th December 2009.
[10] Celik IB, Ghia U, Roache PJ, Freitas CJ, Coleman H, and Raad PE 2008 *Journal of Fluids Engineering* **130(7)** 0780011-4.
[11] Bai CJ, Hsiao FB, Li MH, Huang GY, and Chen YJ 2013 *Procedia Engineering* **67** 279-87.
[12] Edmunds M, Williams AJ, Masters I, and Croft TN. 2017 *Renewable Energy* **101** 67-81.

Acknowledgments

The authors would like to acknowledge the creative mind of Mr Michael Gilbert, the Hydro-Spinna creator.